J Gastroenterol (2016) 51:473–486
DOI 10.1007/s00535-015-1126-4

The Japanese Society of Gastroenterology

ORIGINAL ARTICLE—LIVER, PANCREAS, AND BILIARY TRACT

Comprehensive analyses of mutations and hepatitis B virus integration in hepatocellular carcinoma with clinicopathological features

Fukiko Kawai-Kitahata[1] · Yasuhiro Asahina[1,2] · Shinji Tanaka[3] · Sei Kakinuma[1,2] · Miyako Murakawa[1] · Sayuri Nitta[1] · Takako Watanabe[1] · Satoshi Otani[1] · Miki Taniguchi[1] · Fumio Goto[1] · Hiroko Nagata[1] · Shun Kaneko[1] · Megumi Tasaka-Fujita[1] · Yuki Nishimura-Sakurai[1] · Seishin Azuma[1] · Yasuhiro Itsui[1] · Mina Nakagawa[1] · Minoru Tanabe[4] · Shinichi Takano[5] · Mitsuharu Fukasawa[5] · Minoru Sakamoto[5] · Shinya Maekawa[5] · Nobuyuki Enomoto[5] · Mamoru Watanabe[1]

Received: 5 June 2015 / Accepted: 19 September 2015 / Published online: 9 November 2015

Abstract

Background and Aims Genetic alterations in specific genes are critical events in carcinogenesis and hepatocellular carcinoma (HCC) progression. However, the genetic alterations responsible for HCC development, progression, and survival are unclear.

Methods We investigated the essential difference in genetic alterations between HCC and adjacent non-HCC tissues using next-generation sequencing technology.

Results We found recurrent mutations in several genes such as telomerase reverse transcriptase (*TERT*; 65 % of the total 104 HCCs), *TP53* (38 %), *CTNNB1* (30 %), *AXIN1* (2 %), *PTEN* (2 %), and *CDKN2A* (2 %). *TERT* promoter mutations were associated with older age ($p = 0.005$), presence of hepatitis C virus (HCV) infection ($p = 0.003$), and absence of hepatitis B virus (HBV) infection ($p < 0.0001$). In hepatitis B surface antigen (HBs Ag)-positive HCC without *TERT* promoter mutations, HBV integration into *TERT* locus was found in 47 % patients and was mutually exclusive to *TERT* promoter mutations. Most (89 %) HBV integrants were in the HBx region. *TP53* mutations were associated with HBV infection ($p = 0.0001$) and absence of HCV infection ($p = 0.002$). *CTNNB1* mutations were associated with absence of HBV infection ($p = 0.010$). Moreover, *TERT* promoter mutation was significantly associated with shorter disease-free survival ($p = 0.005$) and poor overall survival ($p = 0.024$).

Conclusions Gene alterations in *TERT* promoter, *TP53*, *CTNNB1*, and HBV integration were closely associated with HCC development, and mutations in *TERT* promoter are related to poor prognosis. These results are useful for understanding the underlying mechanism of hepatocarcinogenesis, diagnosis, and predicting outcomes of patients with HCC.

Keywords *TERT* · *TP53* · *CTNNB1*

Abbreviations

HCC	Hepatocellular carcinoma
TERT	Telomerase reverse transcriptase
HCV	Hepatitis C virus
HBV	Hepatitis B virus

F. Kawai-Kitahata and Y. Asahina contributed equally to this work.

Electronic supplementary material The online version of this article (doi:10.1007/s00535-015-1126-4) contains supplementary material, which is available to authorized users.

✉ Yasuhiro Asahina
asahina.gast@tmd.ac.jp

[1] Department of Gastroenterology and Hepatology, Tokyo Medical and Dental University, 1-5-45 Yushima, Bunkyo-ku, Tokyo 113-8519, Japan

[2] Department of Liver Disease Control, Tokyo Medical and Dental University, 1-5-45 Yushima, Bunkyo-ku, Tokyo 113-8519, Japan

[3] Department of Molecular Oncology, Tokyo Medical and Dental University, 1-5-45 Yushima, Bunkyo-ku, Tokyo 113-8519, Japan

[4] Department of Hepato-Biliary-Pancreatic Surgery, Tokyo Medical and Dental University, 1-5-45 Yushima, Bunkyo-ku, Tokyo 113-8519, Japan

[5] First Department of Internal Medicine, Faculty of Medicine, University of Yamanashi, 1110 Shimogato, Chuo-shi, Yamanshi 409-3898, Japan

HBsAg	Hepatitis B surface antigen
PCR	Polymerase chain reaction
ISPs	Ion sphere particles
COSMIC	Catalogue of somatic mutations in cancer
gDNA	Genomic DNA
CT	Computed tomography
MRI	Magnetic resonance imaging
AFP	Alpha-fetoprotein
DFS	Disease-free survival
OS	Overall survival
Anti-HBc	Antibody to hepatitis B core antigen
Anti-HBs	Antibody to hepatitis B surface antigen

Introduction

Hepatocellular carcinoma (HCC) is the third leading cause of cancer-related deaths worldwide. The major risk factors for HCC are hepatitis B virus (HBV) and hepatitis C virus (HCV) infections, alcohol-induced liver damage, and metabolic diseases [1]. Viral infection or metabolic stress can cause liver damage including fatty change, hepatitis, and cirrhosis. These factors have also been reported to induce genetic and epigenetic damage to the host genome [2]. Recent whole-genome and exome sequencing have identified mutations in *TP53*, Wnt-signaling components *CTNNB1* and *AXIN1*, and several other genes including chromatin regulators *ARID1A*, *ARID2*, and *NFE2L2* in patients with HCC [3–6]. More recently, two independent mutations in the transcriptional regulatory region of the telomerase reverse transcriptase (*TERT*) gene were reported in various cancers including melanoma, glioma, and HCC [7–10]. These mutations create a novel binding site for E-twenty six/ternary complex factor transcription factors and increase promoter activity and *TERT* transcription.

However, the genetic alterations responsible for the development and progression of HCC and the relationship between these mutations and clinicopathological features and prognosis are still unclear. Moreover, the relationship between gene mutations and the etiology of HCC, including HBV and HCV infections and prior to HBV infection, is unknown. Therefore, to clarify the relationship between gene mutations in HCC and its clinicopathological characteristics and patients' prognosis, we investigated the molecular diversity in HCC and adjacent non-HCC tissues using next-generation sequencing technology.

Materials and methods

Patients

One hundred and four patients with HCC who received locally curative hepatectomy at Tokyo Medical and Dental University between December 2001 and July 2014 were included in the present study. Of these patients, 82 were treated as an initial curative hepatectomy for primary HCC. Seventy-eight patients had evidence of hepatitis viral infection (hepatitis B, $n = 28$; or hepatitis C, $n = 50$), 12 patients had alcoholic liver injury, and the remaining 14 patients had unknown etiology as a background liver disease. Characteristics of the patients are shown in Table 1. Written informed consent was obtained from all patients, and the Human Ethics Review Committee of Tokyo Medical and Dental University approved this study, which was conducted in accordance with the Declaration of Helsinki.

DNA preparation and preparation of amplicon libraries

In all 104 patients, tissue samples were immediately obtained after hepatectomy both from HCC and a surrounding non-HCC lesion. After extraction of DNA from these samples by the QIAamp DNA Mini Kit (Qiagen, Valencia, CA, USA), target amplicon libraries were generated by the Ion AmpliSeq Cancer Panel v2 (Life Technologies, Carlsbad, CA, USA), as described previously [11]. In brief, 10 ng of DNA was amplified by polymerase chain reaction (PCR) using premixed Ion AmpliSeq Cancer Primer Pools containing 190 primer pairs and the AmpliSeq HiFi Master Mix (Ion AmpliSeq Library Kit, Life Technologies). The 190 multiplexed amplicons were treated with FuPa Reagent (Life Technologies) for partial digestion of the primer sequences and phosphorylation. The amplicons were then ligated to adapters from the Ion Xpress Barcode Adapters 1–16 Kit or Ion Xpress Barcode Adapters 81–96 Kit (Life Technologies) according to the manufacturer's instructions. After ligation, the amplicons underwent nick-translation and additional library amplification by PCR to complete the linkage between the adapters and amplicons. The BioAnalyzer high-sensitivity DNA kit (Agilent, Santa Clara, CA, USA) was used to visualize the size and range and to determine the library concentrations.

Emulsion PCR and deep sequencing

Multiplexed barcoded libraries were amplified by emulsion PCR on ion sphere particles (ISPs) using the Ion OneTouch 200 Template Kit v2 (Life Technologies) according to the manufacturer's instructions. After the template ISPs were recovered from the emulsion, the positive template ISPs were biotinylated during the emulsion process and enriched with Dynabeads MyOne Streptavidin C1 beads (Life Technologies). Sequencing was performed on a Personal Genome Machine Sequencer (Ion PGM, Life

Table 1 Clinical characteristics of the patients included in the present study

Characteristics	Value
Patients, *n*	104
Gender, *n* (%)	
Male	77 (74.0)
Female	27 (26.0)
Median age (range), year	70 (40–82)
Etiology, *n* (%)	
HBV	28 (26.9)
HCV	50 (48.1)
Alcohol	12 (11.5)
Unknown	14 (13.5)
Tumor number, *n* (%)	
1	77 (74.0)
≥2	27 (26.0)
Median tumor size (range), cm	3.8 (1.3–35)
Non-tumor liver history, *n* (%)	
Normal liver	9 (8.7)
Chronic hepatitis	45 (43.3)
Cirrhosis	50 (48.0)
Child–Pugh class, *n* (%)	
A	95 (91.3)
B	9 (8.7)
Tumor marker	
Median AFP (range), ng/ml	10 (0.5–44,432)
Median PIVKA-II (range), mAU/ml	103 (1–338,000)
Tumor stage, *n* (%)	
I	9 (8.7)
II	46 (44.2)
III	26 (25.0)
IV	23 (22.1)
Tumor differentiation, *n* (%)	
Well differentiated	33 (31.7)
Moderately differentiated	51 (49.0)
Poorly differentiated	20 (19.2)
Vascular invasion, *n* (%)	
Microvascular	37 (35.6)
Macrovascular (large vessel)	11 (10.6)

AFP alpha fetoprotein

Technologies) using the Ion PGM 200 Sequencing Kit (Life Technologies) according to the manufacturer's instructions. Because DNA-mutated tumor cells may exist as minor populations in the samples because of the small proportion among the whole tumor tissues and/or the contamination with nontumor cells, deep sequencing analysis was conducted to detect mutations at a rate as low as 1 %. Torrent Suite software v.4.0.2 (Life Technologies) was used to parse the barcoded reads to align reads to the reference genome and to run metrics, including chip-loading efficiency and total read counts and quality. Variants were identified with Variant Caller v2.0 software (Life Technologies). The quality value of the targeted base was set at 21, which is equal to 0.79 % of the probability for error in mutation detection.

Based on the recent report [12], in which the threshold of the mutation detection ratio was set at 1 %, we set this at 2 % to gain further confidence. The Ion AmpliSeq Cancer Panel v2 (Life Technologies), which was used in library amplification, targets 2790 mutation sites of 50 cancer-related genes that were reported in the Catalogue of Somatic Mutations in Cancer (COSMIC; hotspot mutations) [13]; these detected hotspot mutations were analyzed in combination with the clinical variables. The 50 cancer-related genes are listed in alphabetical order: *ABL1*, *AKT1*, *ALK*, *APC*, *ATM*, *BRAF*, *CDH1*, *CDKN2A*, *CSF1R*, *CTNNB1*, *EGFR*, *ERBB2*, *ERBB4*, *EZH2*, *FBXW7*, *FGFR1*, *FGFR2*, *FGFR3*, *FLT3*, *GNA11*, *GNAQ*, *GNAS*, *HNF1A*, *HRAS*, *IDH1*, *IDH2*, *JAK2*, *JAK3*, *KDR*, *KIT*, *KRAS*, *MET*, *MLH1*, *MPL*, *NOTCH1*, *NPM1*, *NRAS*, *PDGFRA*, *PIK3CA*, *PTEN*, *PTPN11*, *RB1*, *RET*, *SMAD4*, *SMARCB1*, *SMO*, *SRC*, *STK11*, *TP53*, and *VHL*.

The custom primer panel targeting the *ARID1A*, *ARID2*, *AXIN1*, and *NFE2L2* genes (coding exons) was designed using the AmpliSeq Designer. The targeted region was amplified by 50 amplicons (143–275 bp length); 20 ng of genomic DNA (gDNA) was amplified to generate the library using the Ion AmpliSeq Library Kit 2.0.

Nucleotide variants that matched COSMIC and were detected in tumors but were absent in corresponding non-tumor tissue were defined as somatic mutations.

Analysis of *TERT* promoter mutation

TERT promoter mutations were analyzed by direct sequencing. The DNA samples were amplified by PCR using the following pairs of primers encompassing the mutational hotspots (chr5, 1,295,228 C > T and 1,295,250 C > T; hereafter termed C228T and C250T, respectively) in the *TERT* promoter: PCR with primers A (forward): 5′-AGCACCTCGCGGTAGTGG-3′ and primers B (reverse): 5′-CACAGCCTAGGCCGATTC-3′ produce an approximately 500 bp fragment and could then be sequenced with primer A and using a nested primer C (reverse): 5′-GGGCTCCCAGTGGATTC-3′ in the reverse direction.

Design of HBV oligonucleotide probes

To detect the junction point of HBV genome integration into the host genome, 120-mer HBV oligonucleotide probes were designed primarily within the conserved regions of different HBV strains including genotypes Aa, Ae, Ba, Bj, and C, which represent the most common strains found in

Japan. Because we could not totally exclude the possibility of previous exposure of rare genotype, we designed HBV oligonucleotide probes including genotype Aa and Ae. A consensus reference sequence for HBV of each genotype was generated by aligning 41 HBV sequences obtained from the National Center of Biotechnology Information database. To ensure exhaustive coverage of HBV and enrich for all HBV-related sequences whether intact or deleted, a total of 15,545 oligonucleotide probes were designed to span the entire HBV genome at 24 bp apart.

Library preparation and deep sequencing to detect the HBV junction point

The quality of gDNA was assessed on a Nanodrop spectrophotometer (Thermo Fisher Scientific, Wilmington, DE, USA), Qubit Fluorometer (Life Technologies), and 2200 TapeStation (Agilent Technologies). gDNA for HBV genome capture and sequencing was prepared using SureSelectXT2 Target Enrichment System for Illumina Multiplexed Sequencing (Agilent Technologies, Santa Clara, CA, USA), according to the manufacturer's instructions [protocol version D.3 (October 2014)]. Briefly, 100 ng of gDNA was sheared on Covaris (Covaris, Woburn, MA, USA) to a 150–200-bp target size. Sheared fragments were ligated to Illumina's adapters and were enriched by eight cycles of amplification. A total of 1500 ng of amplified libraries were incubated with Agilent's custom capture oligos for 24 h at 65 °C. Hybridized fragments were captured with streptavidin-coated beads, eluted, and amplified by 14 cycles of PCR. Prepared libraries were pooled in batches of 16 and sequenced on a MiSeq (Illumina, San Diego, CA, USA) instrument generating 300-bp paired-end reads.

Sanger sequencing of HBV–human junction breakpoints

To verify HBV–human junction breakpoints detected by above deep sequencing, Sanger sequencing of original genomic DNA without enrichment was performed in the randomly selected HBV integration breakpoints with low junction reads and four representative breakpoints with HBV-TERT junction breakpoint. Sequencing primers were designed based on the paired-end reads, in which one primer was located in the human genome and the other in the HBV genome.

Real-time detection of quantitative PCR analysis for HBV integration breakpoints

To further verify the HBV integration into human genome, copy numbers were measured in the original genomic DNA using SteponePlus Real-Time PCR systems (Life Technologies), and a QuantiTect SYBR Green PCR kit (Qiagen). Copy numbers per cell were normalized to the quantity of beta-2-microglobulin and porphobilinogen deaminase, which have no pseudogenes. The sequences of the primer sets are provided in Supplementary Table 5.

Bioinformatics

After we isolated the paired-end reads, which possibly contained the signals of HBV integration, paired-end read assembly was conducted to obtain reconstructed inserted fragments and to detect HBV integration breakpoints. Low-quality reads were first trimmed using Trimmomatic v0.32 to obtain clean reads for subsequent analysis. Both of the paired-end reads were merged into single sequence using ea-utils fastq-join 1.1.2–537. Merged sequences were aligned to the reference genome (hg19 and HBV) using bwa v0.7.10 (by the BWA-MEM algorithm). The resultant alignment files (SAM format) were converted into BAM format and sorted by chromosomal coordinates using samtools v1.1. From that file, junction reads (i.e., soft-clipped chimeric reads, a part of which was mapped on hg19 and the rest on the HBV genome, indicating a possible integration site) were extracted using custom Perl scripts.

After detecting the junction reads, RefSeq genes were used as the reference database of the human genome. HBV genotyping was performed according to the sequence of junction reads in each sample.

Patient follow-up

After hepatectomy, the patients were examined for HCC recurrence by abdominal ultrasonography, dynamic computed tomography (CT), and/or magnetic resonance imaging (MRI) every 3–6 months. Serum alanine aminotransferase and alpha-fetoprotein (AFP) levels were measured every 1–6 months. Surveillance protocols were in accordance with the standard of care in Japan. If HCC recurrence was suspected on the basis of the screening examination, additional procedures (e.g., dynamic CT, dynamic MRI, CT during hepatic arteriography, CT during arterial portography, contrast-enhanced ultrasonography, and tumor biopsy) were used to confirm the diagnosis. HCC diagnosis was confirmed by needle biopsy, histology of surgically resected specimens, or characteristic radiological findings. Follow-up was between the date of hepatectomy and death or the last medical attendance until October 2014. The mean follow-up period was 34 months (range, 3–102 months).

Statistical analysis

The Chi-square and Fisher's exact tests were used to compare categorical variables between two groups. The

Kruskal–Wallis test was used to analyze the differences between different groups of discrete variables. Survival analyses were performed using Kaplan–Meier's method. Univariate survival analysis was performed using log-rank tests and the Cox's proportional hazards model. Multivariate analyses were conducted using the Cox's proportional hazards model. As covariates in the multivariate stepwise Cox model, the factors that reached statistical significance in univariate survival analyses were included.

Results

Cancer-related mutations in HCC

The cancer-related mutations in the 54 genes were analyzed using Ion Torrent PGM deep sequencing (Ion AmpliSeq Cancer Panel v2 and Ion Ampliseq Custom Panel) in HCC and surrounding non-HCC tissue with an average of 4414 and 2019 reads per amplicon, respectively. The extracted variants with the list of altered genes, variant frequency, read depth, and corresponding COSMIC IDs from the deep-sequencing data of each case are presented in Supplementary Tables 1 and 2. Mutations in *TP53*, *CTNNB1*, *AXIN1*, *CDKN2A*, *PTEN*, *ARID1A*, *ARID2*, *HRAS*, *PIK3CA*, *STK11*, *GNAS*, and *NFE2L2* were found in 39 (37.5 %), 31 (29.8 %), 2 (1.9 %), 2 (1.9 %), 2 (1.9 %), 1 (1.0 %), 1 (1.0 %), 1 (1.0 %), 1 (1.0 %), 1 (1.0 %), 1 (1.0 %), and 1 (1.0 %) of the total 104 HCCs, respectively (Fig. 1a; Table 2, and Supplementary Fig. 1), and 62 (59.6 %) of 104 HCCs had mutations either in *CTNNB1* or in *TP53*. Eight (7.7 %) HCCs had both *CTNNB1* and *TP53* gene mutations, although mutations in these two genes have been reported as a mutually exclusive event [4].

Direct sequencing indicated *TERT* promoter mutations in 68 of 104 HCCs (65.4 %). Of these, 66 (97.0 %) mutations were C228T, whereas two (3.0 %) mutations were C250T. The two hot spot mutations, C250T and C228T, were mutually exclusive, and 66 (97.0 %) were found in C228T. It should be noted that no mutation was detected in the surrounding non-HCC tissue. Ninety-three (89.4 %) of HCC cases had either a mutation in *TP53*, *CTNNB1*, and/or the *TERT* promoter.

Clinicopathological characteristics of HCC according to mutation status

The clinicopathological characteristics according to mutation status were shown in Table 3. *TERT* promoter mutations were associated with older age ($p = 0.005$), HCV infection (59 vs. 28 %; $p = 0.003$), absence of HBV infection (13 vs. 53 %; $p < 0.0001$), and high serum AFP levels ($p = 0.019$). *CTNNB1* mutations were associated with absence of HBV infection (10 vs. 34 %; $p = 0.010$). In contrast, mutations in *TP53* were associated with HBV-related HCC (49 vs. 14 %; $p = 0.0001$) and absence of HCV infection (28 vs. 60 %; $p = 0.002$). Tumor size, tumor number, vascular invasion, and tumor differentiation were not associated with any gene mutations.

Association between HCC gene mutations and disease-free survival or overall survival

Disease-free survival (DFS) and overall survival (OS) were assessed in 82 patients with hepatectomy as an initial curative therapy for primary HCC. During follow-up, there were a total of 49 recurrences for a median DFS of 18.8 months. A total of 26 of 82 (31.7 %) patients died, with a mean OS of 67.8 months with a 5-year OS rate of 59.3 % determined by Kaplan–Meier's analysis. Presence of *TERT* promoter mutations was significantly associated with shorter DFS (median DFS: 16.0 months vs. not reached; $p = 0.005$) and poor OS (median OS: 60.9 months vs. not reached; $p = 0.024$) (Fig. 2; Tables 4, 5). Even in patients with HCV infection, the presence of *TERT* promoter mutations was also significantly associated with shorter DFS (median DFS: 12.3 months vs. not reached, $p = 0.026$) (Supplementary Fig. 2). A trend toward prolonged DFS (median DFS: 18.8 vs. 16.9 months, $p = 0.061$) was observed in patients who were all negative for *TERT*, *TP53*, and *CTNNB1* but did not reach statistical significance because of limited power. There was no significant difference between the presence and absence of mutations in *TP53* (median DFS: 24.5 vs. 16.9 months; $p = 0.974$, median OS: 61.7 vs. 81.3 months; $p = 0.487$) and *CTNNB1* (median DFS; 15.1 vs. 18.8 months; $p = 0.683$, median OS; 81.3 vs. 60.9 months; $p = 0.153$) in DFS or OS (Fig. 2).

Univariate analysis for DFS identified older age ($p = 0.025$), tumor number ($p = 0.002$), vascular invasion ($p = 0.001$), serum levels of PIVKA-II ($p = 0.016$), and presence or absence of *TERT* promoter mutations ($p = 0.005$) as significant predictors. Stepwise multivariate analysis demonstrated that *TERT* promoter mutations, older age, multiple HCC, and vascular invasion were independently associated with shorter DFS (Table 4).

By univariate analysis, age ($p = 0.027$), PIVKA-II ($p = 0.022$), and *TERT* promoter mutations ($p = 0.024$) were significantly associated with OS. By stepwise multivariate analysis, PIVKA-II ($p = 0.046$) and *TERT* promoter mutations ($p = 0.024$) were identified as independent factors associated with poor OS (Table 5).

Breakpoints of HBV integration

Because *TERT* promoter mutations were significantly associated with absence of HBV infection, we further

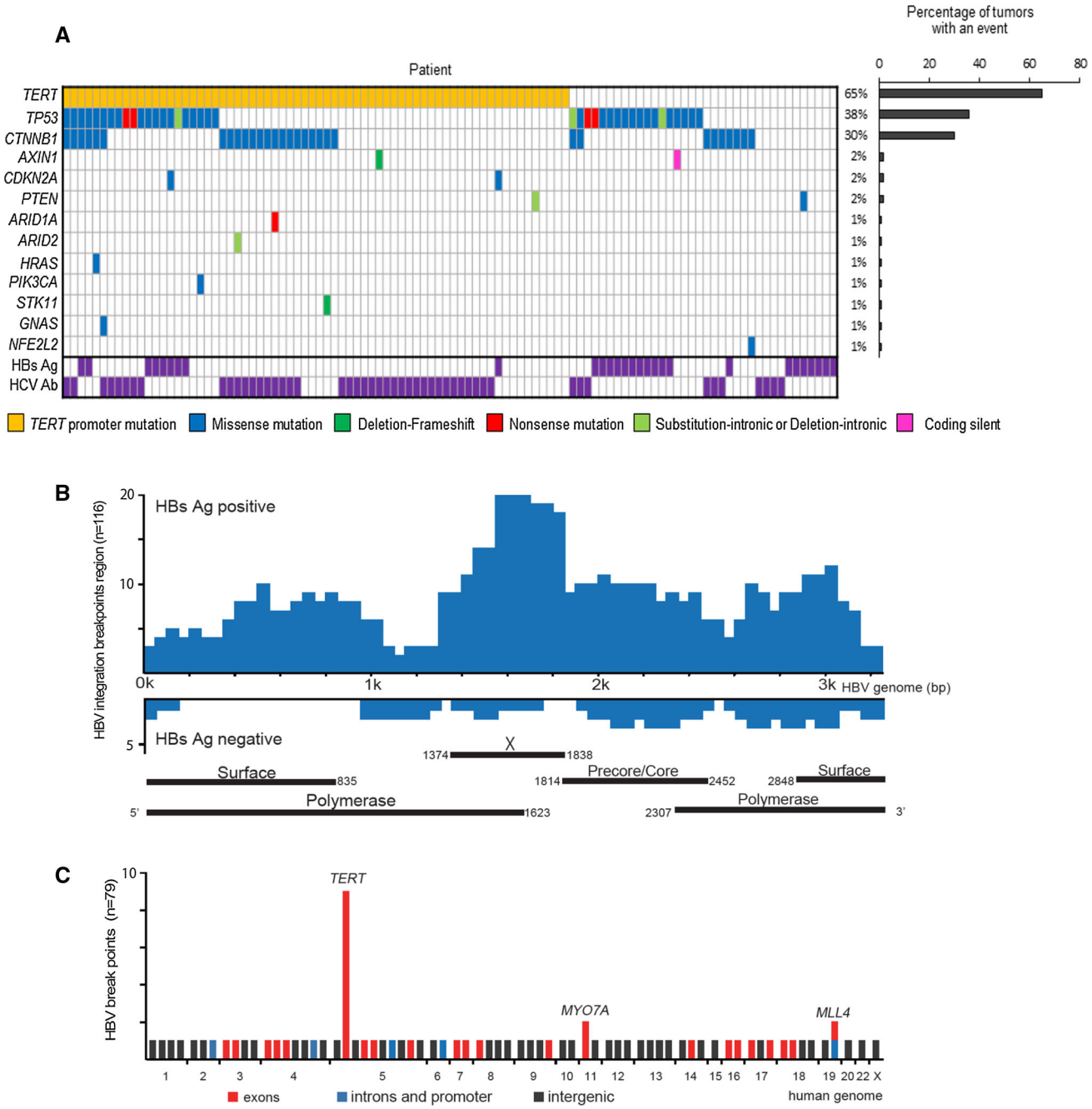

Fig. 1 Overview of somatic mutations in 104 hepatocellular carcinomas (HCCs) and hepatitis B virus (HBV) breakpoints distribution in hepatitis B surface antigen (HBs Ag)-positive HCCs ($n = 28$) and HBsAg-negative/antibody to hepatitis B core antigen (anti-HBc)-positive and/or antibody to hepatitis B surface antigen (anti-HBs)-positive HCCs ($n = 21$). **a** Individual mutations are depicted and color coded by type of mutation. The major clinical features for each tumor are shown with *purple boxes*. **b** Number of integration breakpoints at different sites in the HBV genome. **c** HBV integration breakpoints at a locus in the human genome (hg19) in HBsAg-positive HCCs. Each *bar* represents the number of HBV integration breakpoints. **d** Overview of HBV integration, telomerase reverse transcriptase (*TERT*) promoter mutations, *CTNNB1*, and *TP53* mutations in HBsAg-positive HCC. HBV genome integration into the *TERT* locus and *TERT* promoter mutations are mutual exclusive. One patient whose gDNA library was not available is shown with a *grey box*. **e** Correlation between the number of HBV integrants and age in HBsAg-positive patients with HCC. **f** Overview of HBV integration, *TERT* promoter mutations, *CTNNB1*, and *TP53* mutations in HBsAg-negative/anti-HBc-positive and/or anti-HBs-positive HCC

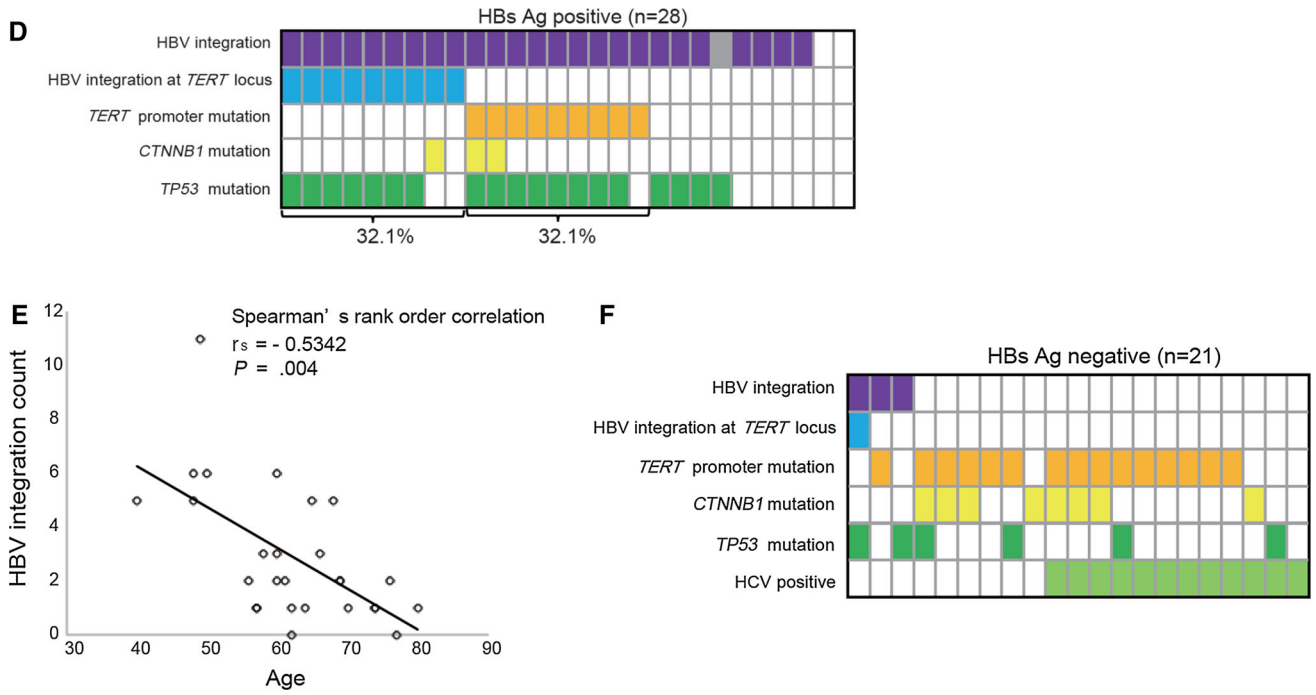

Fig. 1 continued

Table 2 Mutated genes in 104 HCCs

Gene	Total number	No. of patients	No. of sites	Non-silent mutations	Synonymous mutations	SNP	INDEL
TERT	68	68	2	0	68	68	
TP53	45	39	30	42	3	45	
CTNNB1	32	31	7	32	0	32	
AXIN1	3	2	3	1	2	2	1
CDKN2A	2	2	1	2	0	2	
PTEN	2	2	2	1	1	1	1
ARID1A	1	1	1	1	0	1	
ARID2	1	1	1	0	1	1	
HRAS	1	1	1	1	0	1	
STK11	1	1	1	0	1		1
PIK3CA	1	1	1	1	0		1
GNAS	1	1	1	1	0	1	
NFE2L2	1	1	1	1	0	1	

SNP single-nucleotide polymorphism, *INDEL* insertion-deletion

investigated HBV integration in a subgroup of all 49 patients with chronic persistent or prior HBV infection: 28 HBsAg-positive patients and 21 HBsAg-negative and antibody to hepatitis B core antigen (anti-HBc)-positive and/or antibody to hepatitis B surface antigen (anti-HBs)-positive patients. Using paired-end reads mapped to the HBV viral and human genomes, respectively, we obtained an average of 1150 reads supporting HBV integration breakpoints for each sample. In patients HBsAg-positive, a total of 78 HBV integration breakpoints were detected in 25/27 (92.6 %) patients, whereas no HBV integration was observed in two patients. The average integration site in HCC tissues was 2.93 ± 2.5 (mean ± SD) (Supplementary Tables 3, 4). The majority of the patients were integrated with HBV of genotype C ($n = 24$ patients), whereas one patient was infected with HBV of genotype Bj (Supplementary Table 4).

In patients with prior HBV infection, 16 HBV integration breakpoints were detected only in 3/21 (14.3 %)

Table 3 Characteristics of the patients according to gene mutation status ($n = 104$)

Variable	*TERT* promoter mutated ($n = 68$)	*TERT* promoter non mutated ($n = 36$)	p value	*TP53* mutated ($n = 39$)	*TP53* non-mutated ($n = 65$)	p value	*CTNNB1* mutated ($n = 31$)	*CTNNB1* non-mutated ($n = 73$)	p value
Gender									
Male	76 % (52/68)	64 % (23/36)	0.17	67 % (26/39)	78 % (51/65)	0.18	74 % (23/31)	71 % (52/73)	0.76
Female	24 % (16/68)	36 % (13/36)		33 % (13/39)	22 % (14/65)		26 % (8/31)	29 % (21/73)	
Age (years)									
Median (range)	72.0 (40–82)	63.5 (48–82)	0.005*	67.0 (40–80)	71.1 (47–82)	0.17	70.0 (50–81)	69.2 (40–82)	0.82
Etiology									
HBV	13 % (9/68)	53 % (19/36)	<0.0001**	49 % (19/39)	14 % (9/65)	0.0001**	10 % (3/31)	34 % (25/73)	0.01**
HCV	59 % (40/68)	28 % (10/36)	0.003**	28 % (11/39)	60 % (39/65)	0.002**	61 % (19/31)	42 % (31/73)	0.08
Alcohol	15 % (10/68)	6 % (2/36)	0.16	8 % (3/39)	14 % (9/65)	0.42	13 % (4/31)	11 % (8/73)	0.77
Unknown	13 % (9/68)	14 % (5/36)	0.93	15 % (6/39)	12 % (8/65)	0.54	16 % (5/31)	12 % (9/73)	0.60
AFP (ng/ml)									
Median (range)	18.9 (2.0–44432.0)	6.6 (0.5–2495.0)	0.02*	11.2 (0.5–13600.0)	9.9 (2.0–44432.0)	0.76	11.7 (2.3–7960.0)	9.7 (0.5–44432.0)	0.74
PIVKA-II (mAU/ml)									
Median (range)	148.0 (1–338,000)	58.5 1 (1–77,800)	0.18	105.0 (8–77,800)	100.0 (1–338,000)	0.62	65.0 (1–93,500)	105.0 1 (1–338,000)	0.89
Non-tumor liver									
Normal liver	10 % (7/68)	6 % (2/36)	0.71	10 % (4/39)	8 % (5/65)	0.72	6 % (2/31)	10 % (7/73)	0.87
Chronic hepatitis	43 % (29/68)	44 % (16/36)		38 % (15/39)	46 % (30/65)		45 % (14/31)	42 % (31/73)	
Cirrhosis	47 % (32/68)	50 % (18/36)		51 % (20/39)	46 % (30/65)		48 % (15/31)	48 % (35/73)	
Tumor number									
Single	72 % (49/68)	78 % (28/36)	0.53	74 % (29/39)	74 % (48/65)	0.95	77 % (24/31)	73 % (53/73)	0.61
Multiple	28 % (19/68)	22 % (8/36)		26 % (10/39)	26 % (17/65)		23 % (7/31)	27 % (20/73)	
Tumor size (cm)									
Median (range)	3.7 (1.5–35.0)	3.8 (1.3–15.0)	0.63	4.0 (1.5–35.0)	3.5 (1.3–19.0)	0.46	3.7 (1.4–19.0)	3.8 (1.3–35.0)	0.33
Tumor differentiation									
Well	35 % (24/68)	25 % (9/36)	0.53	28 % (11/39)	34 % (22/65)	0.07	29 % (9/31)	33 % (24/73)	0.92
Moderately	46 % (31/68)	56 % (20/36)		41 % (16/39)	54 % (35/65)		52 % (16/31)	48 % (35/73)	
Poorly	19 % (13/68)	19 % (7/36)		31 % (12/39)	12 % (8/65)		19 % (6/31)	19 % (14/73)	
Vascular invasion									
Yes	46 % (31/68)	44 % (16/36)	0.91	54 % (21/39)	40 % (26/65)	0.33	42 % (13/31)	47 % (34/73)	0.66
No	54 % (37/68)	56 % (20/36)		46 % (18/39)	60 % (39/65)		58 % (18/31)	53 % (39/73)	

Table 3 continued

Variable	*TERT* promoter mutated ($n = 68$)	*TERT* promoter non mutated ($n = 36$)	p value	*TP53* mutated ($n = 39$)	*TP53* non-mutated ($n = 65$)	p value	*CTNNB1* mutated ($n = 31$)	*CTNNB1* non-mutated ($n = 73$)	p value
Stage									
I	7 % (5/68)	11 % (4/36)	0.73	8 % (3/39)	9 % (6/65)	0.92	0 % (0/31)	12 % (9/73)	0.11
II	44 % (30/68)	44 % (16/36)		44 % (17/39)	45 % (29/65)		52 % (16/31)	41 % (30/73)	
III	24 % (16/68)	28 % (10/36)		23 % (9/39)	26 % (17/65)		32 % (10/31)	22 % (16/73)	
IV	25 % (17/68)	17 % (6/36)		26 % (10/39)	20 % (13/65)		16 % (5/31)	25 % (18/73)	

p values obtained from Kruskal–Wallis (*) and Chi-squared (**) tests based on the given clinical variable are shown

patients, and all of three patients were negative for antibody to hepatitis C virus (anti-HCV). All patients were integrated with HBV genotype C ($n = 3$ patients).

Characteristics of HBV integration breakpoints

To investigate the distribution pattern of integration sites in the human genome, we examined the HBV integration breakpoints in 94 nonrepetitive integration sites including 95 in human genome and 120 different loci in the HBV genome. In HBsAg-positive patients, 21 of 78 (37.2 %) sites were located in gene-coding regions (including exons and introns). Within the HBV genome, 34 of 78 (43.6 %) were observed in a 550 bp region from 1300 to 1850 bp, where the HBx gene and the initiation site of viral replication and transcription are located [14–16] (Fig. 1b). HBV integration was frequently found in particular genes including *TERT* ($n = 9$), *KMT2B* (*MLL4*; $n = 2$), and *MYO7A* ($n = 2$) (Fig. 1c). Seven (77.8 %) of *TERT* locus breakpoints were paired with HBx gene, all at the 3′-end of HBx gene. Eight of *TERT* locus breakpoints were found to reside-55 and 2214 upstream of *TERT* TSS, whereas 1 *TERT* locus was located in an intron. HBV genome integration in the *TERT* locus was mutually exclusive with *TERT* promoter mutation in HBsAg-positive samples (Fig. 1d). We also examined the association between clinical parameters and the number of HBV integrations per tumor. The HBV integration number was significantly associated with HCC at younger age (Spearman's rank order correlation, $r_s = -0.5342$, $p < 0.01$) (Fig. 1e).

In 21 patients with prior HBV infection, a total of 16 integration sites were detected. Eight of 16 (50.0 %) sites were located in gene-coding regions (including exons and introns). Breakpoints were randomly distributed through the HBV genome, and only two of 16 (12.5 %) were found in the HBx gene (Fig. 1b). In one patient, the HBV genome was integrated into the *TERT* gene, which event was also mutually exclusive with *TERT* promoter mutation (Fig. 1f).

Confirmation of HBV integration into human genome

Integration of HBV into the human genome was confirmed by Sanger sequence in original genomic DNA in ten HBV integration breakpoints with low junction reads and four representative breakpoints with HBV-*TERT* junction (Supplementary Fig. 3). Copy numbers of HBV-human chimeric DNA were successfully quantified in three of four representative patients with HBV integration breakpoints in *TERT* locus. As a result, percentages of threshold cycles of HBV-*TERT* chimeric DNA normalized by control genes were 26.9–56.7 %. Since HBV integration into human host chromosomes usually occurs in one allele, these results

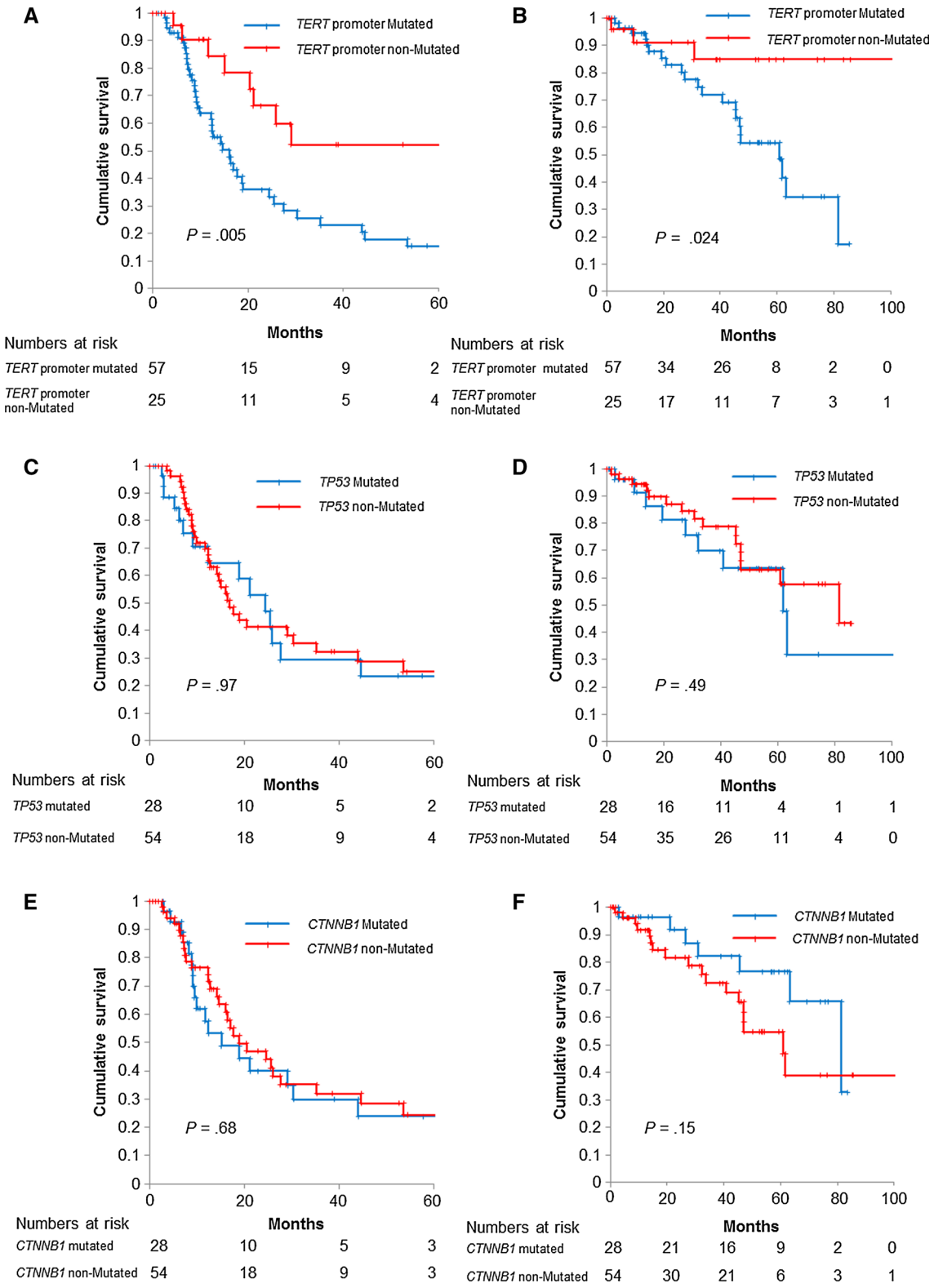

Fig. 2 **a**, **b** Disease-free survival (DFS) curves and overall survival (OS) curves according to telomerase reverse transcriptase promoter mutation status evaluated by Kaplan–Meier method. **c**, **d** DFS and OS curves according to *TP53* mutation status evaluated by Kaplan–Meier method. **e**, **f** DFS and OS curves according to *CTNNB1* mutation status evaluated by Kaplan–Meier method. The number of patients at risk at each time point is shown below the graphs

Table 4 Predictors of disease-free survival

	Median DFS (months; 95 % CI)	Univariate analysis		Multivariate analysis	
		HR (95 % CI)	*p* value	HR (95 % CI)	*p* value
TERT					
Non-mutated	Not reached	1			
Mutated	16.0 (11.5–20.6)	0.33 (0.15–0.71)	0.005	0.46 (0.21–0.99)	0.049
TP53					
Non-mutated	16.9 (12.3–21.5)	1			
Mutated	24.5 (16.0–32.9)	1.00 (0.55–1.85)	0.97		
CTNNB1					
Non-mutated	18.8 (8.3–29.4)	1			
Mutated	15.1 (4.3–25.8)	0.88 (0.49–1.56)	0.68		
Gender					
Female	21.2 (13.0–29.3)	1			
Male	18.8 (12.6–25.1)	0.94 (0.46–1.94)	0.85		
Age		1.04 (1.00–1.07)	0.025	1.04 (1.00–1.07)	0.029
Tumor number					
Single	25.5 (15.1–35.8)	1			
Multiple	9.1 (5.3–12.8)	0.37 (0.20–0.70)	0.002	0.66 (0.47–0.93)	0.017
Tumor size		1.03 (0.98–1.07)	0.26		
HBV					
Negative	16.4 (11.9–20.9)	1			
Positive	25.9 (0.0–53.0)	1.81 (0.81–4.05)	0.15		
HCV					
Negative	25.9 (13.6–38.2)	1			
Positive	15.1 (10.7–19.4)	0.70 (0.39–1.23)	0.21		
Tumor differentiation					
Well	35.2 (10.5–59.9)	1			
Moderately	17.7 (12.4–22.9)	1.59 (0.773.29)	0.21		
Poorly	12.4 (4.6–20.1)	2.31 (0.98–5.45)	0.057		
Vascular invasion					
Negative	44.6 (7.4–81.8)	1			
Positive	12.4 (6.6–18.2)	0.36 (0.20–0.64)	0.001	0.68 (0.50–0.93)	0.014
Non-tumor liver					
Normal liver	14.6 (4.6–24.7)	1			
Chronic hepatitis	25.4 (10.6–40.3)	0.90 (0.34–2.39)	0.84		
Cirrhosis	18.8 (15.4–22.3)	0.96 (0.36–2.55)	0.93		
Stage					
I	44.6 (0.0–98.2)	3.33 (0.75–14.28)	0.11		
II	35.2 (0.0–72.1)	3.44 (1.67–7.14)	0.001		
III	16.0 (10.0–22.0)	1.51 (0.74–3.03)	0.25		
IV	7.4 (4.7–10.0)	1			
AFP		1.01 (1.00–1.00)	0.96		
PIVKA-II		1.00 (1.00–1.00)	0.016		0.28

HR hazard ratio by Cox's proportional hazards model

suggest copy numbers of HBV-*TERT* chimeric DNAs are approximately one copy per cell. Taken together, HBV integration into the *TERT* locus detected by deep sequencing is unlikely to be an artificial one.

Discussion

In the present study, we comprehensively analyzed the mutation status in 104 paired HCC and non-HCC tissue using next-generation sequencing. We identified the mutation frequency of *TP53* (38 %), *CTNNB1* (35 %), *AXIN1* (2 %), *PTEN* (2 %), *CDKN2A* (2 %), and *TERT* promoter mutation (65 %). *TERT*, *TP53*, and *CTNNB1* were the most frequently altered genes and almost 90 % of 104 HCCs had mutations in the *TERT* promoter, *TP53*, or *CTNNB1*.

We also found that these genes were closely associated with the etiology of HCC. Consistent with recent studies [8, 17], we further confirmed the following associations: *TERT* promoter mutations were associated with the presence of HCV infection and absence of HBV infection; *TP53* mutations were associated with HBV infections and absence of HCV infection; and *CTNNB1* mutations were associated with absence of HBV infection. These results suggest that genomic features and the underlying pathway responsible for hepatocarcinogenesis, which may influence the treatment strategy, were substantially different between HBV-related and HCV-related HCC. Moreover, we demonstrated for the first time that the *TERT* promoter mutation itself is closely associated with a poor prognosis in both DFS and OS, which was independent from tumor characteristics such as tumor differentiation and vascular invasion. Because most HCC recurrence observed was estimated as a multicentric occurrence and no *TERT* promoter mutations were found in the corresponding non-HCC tissue, patients with some status of the background liver, in which new *TERT* mutations tend to easily occur, may cause earlier de novo HCC recurrence. Because *TERT* mutations are thought to be an early event in hepatocarcinogenesis [18], such status of the background liver may responsible for poor prognosis. Although further investigation is needed to prove this hypothesis, our data, which addresses the association between gene mutation and prognosis, are useful in making a decision for postoperative surveillance strategies or the timing of liver transplantation in individual patients.

We also found that HCC with *TERT* promoter mutations were closely associated with older age. Because chronic HBV infection is mostly caused by vertical or horizontal transmission during infancy in Japan, the average age of patients with HBV-related HCC is lower than that in patients with HCV-related HCC [19–22], which is one of the possible reasons for the association of *TERT* promoter mutations with older age. However, because the poor prognosis of HCC with *TERT* promoter mutations was also found even in HCV-related HCC, and our multivariate analysis demonstrated that *TERT* promoter mutation was identified as an independent factor that was associated with poor prognosis, it is unlikely that poor prognosis related to *TERT* promoter mutation was a surrogate of age or etiology of HCC.

We investigated HBV integration using paired-end deep sequencing to address whether the lower rate of *TERT* promoter mutation in HBV-related HCC could be explained by the preference of HBV integration in the *TERT* promoter region, which was known to induce transcriptional activation of *TERT* [15, 23]. We found HBV integration in 92.6 % (25 of 27) of the HBsAg-positive patients, and 47 % (eight of 19) of them without *TERT* promoter mutations were found in the *TERT* locus. Interestingly, HBV genome integrations in the *TERT* locus were mutually exclusive with *TERT* promoter mutations. Either hotspot *TERT* promoter mutations or viral integration occurs in more than 64 % of the HBsAg-positive patients, suggesting *TERT* as an important role of hepatocarcinogenesis. We also characterized the integrated HBV genome in patients with HCC. The preferential site within the HBV genome that integrates into the human genome was found to reside around 1300–1850 bp, where the viral enhancer, X gene, and core gene are located. In addition, we disclosed the frequent integration at the 3′ end of HBx in the *TERT* gene and *TERT* locus breakpoints located in promoter were found to reside −55 and 2214 upstream of the *TERT* TSS. Because the expression of the *TERT* gene correlates with the distance of integration sites from the TSS and only when the site of integration is at the 3′ end of HBx are chimeric transcripts observed [24], HBx integration to the *TERT* locus is likely responsible for hepatocarcinogenesis in patients with HCC without *TERT* promoter mutations. Moreover, because we also found that the number of HBV integrants was associated with younger age, it is likely that the number of integrations may have a role in early events in hepatocarcinogenesis.

In contrast, HBV integration was detected in only three of 21 (14.3 %) patients with prior HBV infection (HBsAg-negative and anti-HBc- and/or anti-HBs-positive patients), and only one breakpoint was located in *TERT* gene. Although a contribution of HBV infection to the development of HCC is likely in this particular patient, lower rate of HBV integration events and the different integration pattern on the HBV genome in patients with prior HBV infection suggests that mechanism responsible for hepatocarcinogenesis could be different between patients with chronic HBV infection and prior infection. Because *TERT* promoter mutation was found in 71 % (15/21) of the

Table 5 Predictors of overall survival

	Median OS (months; 95 % CI)	Univariate analysis		Multivariate analysis	
		HR (95 % CI)	*p* value	HR (95 % CI)	*p* value
TERT					
Non-mutated	Not reached	1			
Mutated	60.9 (44.2–77.5)	0.50 (0.27–0.91)	0.024	0.25 (0.07–0.83)	0.024
TP53					
Non-mutated	81.3 (41.9–120.8)	1			
Mutated	61.7 (39.6–83.9)	0.87 (0.58–1.30)	0.49		
CTNNB1					
Non-mutated	60.9 (45.2–76.5)	1			
Mutated	81.3 (55.2–107.5)	1.37 (0.88–2.13)	0.15		
Gender					
Female	Not reached	1			
Male	81.3 (52.4–110.2)	1.36 (0.87–2.11)	0.17		
Age		1.06 (1.01–1.11)	0.027		0.074
Tumor number					
Single	81.3 (53.3–109.4)	1			
Multiple	81.3 (51.8–110.9)	0.75 (0.48–1.16)	0.19		
Tumor size		1.03 (0.96–1.10)	0.44		
HBV					
Negative	63.1 (48.5–77.8)	1			
Positive	Not reached	1.14 (0.67–1.96)	0.63		
HCV					
Negative	Not reached	1			
Positive	63.1 (35.6–90.7)	0.84 (0.56–1.25)	0.39		
Tumor differentiation					
Well	81.3 (30.5–132.1)	1			
Moderately	63.1 (20.5–105.8)	1.07 (0.61–1.87)	0.81		
Poorly	60.9 (41.1–80.7)	1.16 (0.58–2.31)	0.68		
Vascular invasion					
Negative	81.3 (54.3–108.4)	1			
Positive	Not reached	0.75 (0.34–1.68)	0.49		
Non-tumor liver					
Normal liver	Not reached	1			
Chronic hepatitis	Not reached	0.61 (0.13–2.84)	0.53		
Cirrhosis	61.7 (37.2–86.2)	1.01 (0.23–4.53)	0.98		
Stage					
I	Not reached	N/A	0.98		
II	63.1 (49.8–76.4)	2.00 (0.79–5.00)	0.14		
III	Not reached	3.33 (1.05–10.00)	0.04		
IV	47.0 (25.3–68.8)	1			
AFP		1.00 (1.00–1.00)	0.52		
PIVKA-II		1.00 (1.00–1.00)	0.022	1.00 (1.00–1.00)	0.046

HR hazard ratio by Cox's proportional hazards model, *N/A* not available due to no censor deaths

patients with prior HBV infection, the mechanism for the development of HCC in patients with prior HBV infection could be similar to that in patients without any evidence for HBV infection.

This study has a limitation. As presented in Supplementary Tables 1 and 2, 52 mutations were found in genes such as *TP53*, *PTEN*, and *APC* in both of HCC and non-HCC tissue using COSMIC as a reference. Hence, these

mutations could be associated with hepatocarcinogenesis at an early stage of HCC, and may underestimate the influence of existing important mutations, because buffy coat was not used as a reference. However, as most gene mutations in both of HCC and non-HCC tissue were common among patients and variant frequencies of these gene mutations were often multiples of "25" or "33", these could be single-nucleotide polymorphisms in Japanese.

In conclusion, gene alterations in *TERT* promoter, *TP53*, and *CTNNB1* are closely associated with HCC development, and mutations in *TERT* promoter are related to poor prognosis. *TERT* promoter mutations and HBV integration into *TERT* locus are independently associated with hepatocarcinogenesis in HBsAg-positive patients. The present results provide useful information for understanding the mechanism of hepatocarcinogenesis and have potentially important clinical implications that may influence diagnostic decisions and treatment strategies in individual patients.

Compliance with ethical standards

Conflict of interest Dr. Asahina and Dr. Kakinuma belong to a donation-funded department funded by Chugai Pharmaceutical Co. Ltd., Toray Industries Inc., Bristol-Myers Squibb, Dainippon Sumitomo Pharma Co. Ltd., and Merck Sharp & Dohme. The others have nothing to disclose.

Financial Support This study was supported by grants from the Japanese Ministry of Education, Culture, Sports, Science, and Technology; the Japanese Ministry of Welfare, Health, and Labor; the Japan Society for the Promotion of Science; and the Japan Health Sciences Foundation.

References

1. El-Serag HB. Epidemiology of viral hepatitis and hepatocellular carcinoma. Gastroenterology. 2012;142(1264–73):e1.
2. Thorgeirsson SS, Grisham JW. Molecular pathogenesis of human hepatocellular carcinoma. Nat Genet. 2002;31:339–46.
3. Huang J, Deng Q, Wang Q, et al. Exome sequencing of hepatitis B virus-associated hepatocellular carcinoma. Nat Genet. 2012;44:1117–21.
4. Guichard C, Amaddeo G, Imbeaud S, et al. Integrated analysis of somatic mutations and focal copy-number changes identifies key genes and pathways in hepatocellular carcinoma. Nat Genet. 2012;44:694–8.
5. Fujimoto A, Totoki Y, Abe T, et al. Whole-genome sequencing of liver cancers identifies etiological influences on mutation patterns and recurrent mutations in chromatin regulators. Nat Genet. 2012;44:760–4.
6. Li M, Zhao H, Zhang X, et al. Inactivating mutations of the chromatin remodeling gene ARID2 in hepatocellular carcinoma. Nat Genet. 2011;43:828–9.
7. Killela PJ, Reitman ZJ, Jiao Y, et al. TERT promoter mutations occur frequently in gliomas and a subset of tumors derived from cells with low rates of self-renewal. Proc Natl Acad Sci USA. 2013;110:6021–6.
8. Nault JC, Mallet M, Pilati C, et al. High frequency of telomerase reverse-transcriptase promoter somatic mutations in hepatocellular carcinoma and preneoplastic lesions. Nat Commun. 2013;4:2218.
9. Huang FW, Hodis E, Xu MJ, Kryukov GV, Chin L, Garraway LA. Highly recurrent TERT promoter mutations in human melanoma. Science. 2013;339:957–9.
10. Horn S, Figl A, Rachakonda PS, et al. TERT promoter mutations in familial and sporadic melanoma. Science. 2013;339:959–61.
11. Beadling C, Neff TL, Heinrich MC, et al. Combining highly multiplexed PCR with semiconductor-based sequencing for rapid cancer genotyping. J Mol Diagn. 2013;15:171–6.
12. Takano S, Fukasawa M, Maekawa S, et al. Deep sequencing of cancer-related genes revealed GNAS mutations to be associated with intraductal papillary mucinous neoplasms and its main pancreatic duct dilation. PLoS One. 2014;9:e98718.
13. Forbes SA, Bindal N, Bamford S, et al. COSMIC: mining complete cancer genomes in the catalogue of somatic mutations in cancer. Nucleic Acids Res. 2011;39:D945–50.
14. Jiang Z, Jhunjhunwala S, Liu J, et al. The effects of hepatitis B virus integration into the genomes of hepatocellular carcinoma patients. Genome Res. 2012;22:593–601.
15. Sung WK, Zheng H, Li S, et al. Genome-wide survey of recurrent HBV integration in hepatocellular carcinoma. Nat Genet. 2012;44:765–9.
16. Li X, Zhang J, Yang Z, et al. The function of targeted host genes determines the oncogenicity of HBV integration in hepatocellular carcinoma. J Hepatol. 2014;60:975–84.
17. Chen YL, Jeng YM, Chang CN, et al. TERT promoter mutation in resectable hepatocellular carcinomas: a strong association with hepatitis C infection and absence of hepatitis B infection. Int J Surg. 2014;12:659–65.
18. Nault JC, Calderaro J, Tommaso LD, et al. Telomerase reverse transcriptase promoter mutation is an early somatic genetic alteration in the transformation of premalignant nodules in hepatocellular carcinoma on cirrhosis. Hepatology. 2014;60:1983–92.
19. Ng J, Wu J. Hepatitis B- and hepatitis C-related hepatocellular carcinomas in the United States: similarities and differences. Hepat Mon. 2012;12:e7635.
20. Sasaki Y, Yamada T, Tanaka H, et al. Risk of recurrence in a long-term follow-up after surgery in 417 patients with hepatitis B- or hepatitis C-related hepatocellular carcinoma. Ann Surg. 2006;244:771–80.
21. Minami T, Tateishi R, Shiina S, et al. Comparison of improved prognosis between hepatitis B- and hepatitis C-related hepatocellular carcinoma. Hepatol Res. 2015;45:E99–107.
22. Takenaka K, Yamamoto K, Taketomi A, et al. A comparison of the surgical results in patients with hepatitis B versus hepatitis C-related hepatocellular carcinoma. Hepatology. 1995;22:20–4.
23. Paterlini-Bréchot P, Saigo K, Murakami Y, et al. Hepatitis B virus-related insertional mutagenesis occurs frequently in human liver cancers and recurrently targets human telomerase gene. Oncogene. 2003;22:3911–6.
24. Toh ST, Jin Y, Liu L, et al. Deep sequencing of the hepatitis B virus in hepatocellular carcinoma patients reveals enriched integration events, structural alterations and sequence variations. Carcinogenesis. 2013;34:787–98.